Reverse magnetostructural transformation and adiabatic temperature change in Co- and In-substituted Ni-Mn-Ga alloys

G. Porcari,[1,*] S. Fabbrici,[2,3] C. Pernechele,[1] F. Albertini,[3] M. Buzzi,[1] A. Paoluzi,[3] J. Kamarad,[4] Z. Arnold,[4] and M. Solzi[1]

[1]*Dipartimento di Fisica and CNISM, Università di Parma, v.le G.P. Usberti 7/A, I-43100 Parma, Italy*

[2]*MIST E-R Laboratory, via Gobetti 101, I-40129 Bologna, Italy*

[3]*IMEM-CNR, Parco Area delle Scienze 37/A, I-43100 Parma, Italy*

[4]*Institute of Physics ASCR, v.v.i. Na Slovance 2, 182 21 Praha 8, Czech Republic*

(Received 27 July 2011; revised manuscript received 23 December 2011; published 12 January 2012)

A careful characterization of the magnetocaloric effect in Co-substituted Ni-Mn-Ga Heusler alloys, based both on direct and indirect methods, is presented. In the present paper, adiabatic temperature change values (ΔT_{ad}) up to 1.6 K in 1.9 T were measured across the magnetostructural transformations. The studied samples, with similar transformation temperatures and comparable entropy changes, show surprising differences of the ΔT_{ad}. In order to gain better insight into the behavior of the ΔT_{ad} peak values among different samples, a qualitative model is proposed based on magnetization and magnetothermal data.

DOI: 10.1103/PhysRevB.85.024414 PACS number(s): 75.30.Sg, 75.50.Cc

I. INTRODUCTION

The magnetocaloric effect (MCE) is an intrinsic response of magnetic materials to a change of external magnetic field. This action on the magnetic structure induces an adiabatic temperature variation, $\Delta T_{ad}(H,T)$, or an isothermal entropy change,[1] $\Delta s_{isoT}(H,T)$. The effect is expected to be maximum in the proximity of second-order magnetic order-disorder transitions as well as across first-order magnetostructural or metamagnetic transformations:[2,3] up to now, the Δs_{isoT} deduced from magnetization or calorimetric measurements is the usually studied property in order to characterize the MCE.[4] However, a direct correlation between large Δs_{isoT} and high ΔT_{ad} values is not always straightforward, especially when dealing with first-order transformations, where artifact values of the entropy change arising from the presence of hysteretic phenomena have to be taken into account.[5,6] A proper comparison of the magnetocaloric properties of different samples based on the Δs_{isoT} values should be limited to similar systems and across processes occurring at comparable temperatures.[4] Nonetheless, quantitative evaluation of ΔT_{ad} values from indirect measurements relies on the heat capacity[4] $c_p(H,T)$, which should be properly measured.[7] Concerning the search for empirical key features related to the improvement of the MCE in first-order processes, it has been shown that high adiabatic temperature changes are linked to a high sensitivity of the transition temperature (T_M) as a function of the applied field[2] ($|\Delta T_M|/\mu_0\Delta H$), and that a high magnetization variation among the two phases involved in the transformation ($|\Delta M|$) contributes to enhance the inverse MCE.[6,8]

Among the most promising materials, as far as the development of active magnetic regenerators is concerned,[1,9] a peculiar role is played by the Ni-Mn-X Heusler alloys (X = In, Ga, Sn),[10,11] which show a magnetostructural martensitic first-order transformation between a high-temperature cubic austenite and a low-temperature martensite of reduced symmetry.[12] The possibility, by suitably varying the composition, to change both the structural[13] and the magnetic properties,[14] together with the critical temperature of the reversible transformation (T_M), makes these alloys very attractive for a variety of applications: previous studies highlighted their magnetoelastic behavior,[8,15] which could be exploitable in innovative sensors and actuators.[12,16] Concerning the magnetocaloric properties, viable experimental routes for enhancing both the direct[17] and the inverse MCE[18] have been developed, involving the merging of the structural and the magnetic critical temperatures. Previous works have demonstrated the possibility to induce a concurrent magnetostructural transformation from ferromagnetic martensite to paramagnetic austenite in Mn-rich Ni-Mn-Ga.[19] Subsequently, the partial substitution of Ni by Co in Mn-rich alloys was found to selectively lower the resulting magnetic moments in the martensitic phase while strengthening the ferromagnetic interactions of austenite.[20] This feature allowed for the realization of a reverse magnetostructural transformation from paramagnetic martensite to ferromagnetic austenite, enabling high values of $|\Delta M|$ at the T_M and of $|\Delta T_M|/\mu_0\Delta H$. The phase diagram resulting from this substitution on the structural and magnetic critical temperatures as well as the magnetic properties has recently been shown.[21,22]

By affecting the structural and magnetic critical temperatures differently, Co substitution establishes two different regimes, depending on composition. For lower Co and Mn content, the martensitic transformation occurs between two ferromagnetic phases, while in Co- and Mn-rich samples, a paramagnetic gap between martensite and austenite is found, owing to the lowering of the Curie temperature of the martensitic phase well below the T_M itself. In such samples, a dramatic increase of $|\Delta M|$ and $|\Delta T_M|/\mu_0\Delta H$ occurs, while the martensitic transformation is always realized at quite high temperatures ($T_M > 380$ K).[22] The lowering of the T_M while preserving the magnetic properties can be obtained by homovalent partial substitution of the sp element, as shown by Aksoy and co-workers in Ni-Mn-(Ga,In) samples.[23]

The aim of the present paper is to describe and discuss the MCE behavior of two Ni-Co-Mn-(Ga,In) samples (with and without the presence of a paramagnetic gap) displaying the T_M at similar temperatures and representative of the two different regimes described above.

For the sake of simplicity in this paper, the alloy characterized by a lower ΔM at the transformation between two ferromagnetic phases will be labeled *Sample A*. The alloy displaying the paramagnetic gap and the higher ΔM will be named *Sample B*.

The martensitic transformations are first-order irreversible magnetostructural processes characterized by hysteresis. Ideal first-order processes are described by the Clausius-Clapeyron relation,

$$\mu_0 \frac{dH}{dT} = -\frac{\Delta s}{\Delta M}. \quad (1)$$

Real first-order processes, on the other hand, occur in finite temperature or magnetic-field intervals, being far from step-like, so that the $(\partial M/\partial T)_H$ parameter does not diverge. Thus the integration of the isothermal curves required by the use of the Maxwell relation,

$$\Delta s = \mu_0 \int_{H_i}^{H_f} \left(\frac{\partial M}{\partial T}\right)_H dH, \quad (2)$$

if properly probed, turns out to be analytically allowed.[5] It is difficult to understand where the limit lies that establishes the reliability of one of the two approaches. For this reason, in this work we decided to report both values related to the two relations.

The importance of performing direct adiabatic temperature change measurements in order to properly study the MCE of Heusler alloys has been underlined. Moya and co-workers[24] stressed that it is difficult to accurately calculate the adiabatic temperature change by indirect and calorimetric measurements using $\Delta T_{ad} = (T/c_p)\Delta s_{isoT}$ deduced from the Maxwell relations.

In order to allow for a better understanding of the correlations between the properties of the martensitic irreversible process, a geometrical construction (Fig. 1) provides a schematic graphical representation of the temperature-dependent entropy curves with and without an applied magnetic field. Due to the inverse MCE, it is expected that the strongest adiabatic temperature change is realized on the heating branch of the first-order process rather than on the cooling one; thus, we will focus our analysis on the martensite to austenite path of the transformation. For this reason also, the entropy diagram of Fig. 1 describes only the heating curves. The dummy $s(T)$ curves (expressed in arbitrary units) mimicking the shape of the martensitic transformation directly measured in the $M(T)$ curves can be constructed if the phase fraction in the transition region is chosen as the order parameter of the process.[25] This construction makes the presented graphical model (Fig. 1) significant only in the transition region, where the critical temperatures marking the starting and finishing points of the transformation in the $s(T)$ curves are assumed to coincide with those deduced by the magnetothermal characterization. The construction helps to connect some features of the martensitic process, namely the ΔT_{ad} and the Δs_{isoT} peak values with the $\Delta T_M/\mu_0 \Delta H$ and the c_p value characteristic of the martensitic phase.

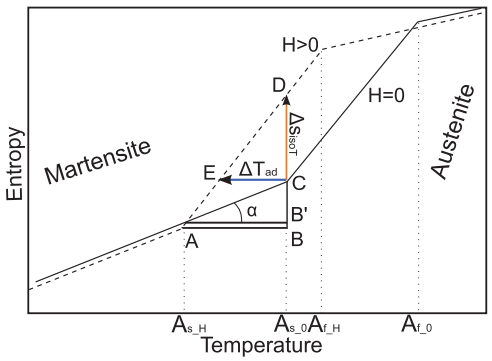

FIG. 1. (Color online) Geometrical construction of the first-order martensitic process in the s vs T plane. The behavior of ΔT_{ad} peak value in the two samples can be roughly estimated from Δs_{isoT} peak values obtained from $M(H)$ curves also considering the c_p of the martensite below the transformation region.

II. EXPERIMENTAL

The samples studied in this work were prepared by arc melting the stoichiometric amounts of pure elements and were subsequently homogenized by annealing at 900 °C for 72 h. $M(T)$ isofield measurements as well as $M(H)$ isothermal curves on heating were performed using an MPMS Quantum Design SQUID magnetometer, stabilizing the temperature before each measurement. ΔT_{ad} was evaluated applying fields up to 1.90 ± 0.05 T in an electromagnet with a maximum field rate of ~2.2 T/s. The probe used to perform the direct measurements of adiabatic temperature change was built using a Cernox HT-BR temperature sensor, the response of which is mostly independent of the external magnetic fields. Its mass ($m \sim 3$ mg) and its time response ($t_s \sim 135$ ms at room temperature) guarantee the possibility to perform accurate and fast measurements. The sensor chip was fixed with an epoxy resin in a rigid housing to avoid mechanical stresses on the Cernox during the measurement when the sample is attached to it. To improve the adiabaticity of the system, the measurements were done in a purpose-built chamber able to guarantee a maximum vacuum level of $P \sim 10^{-4}$ mbar, while a thermoconductive paste was used to improve the thermal contact. Preliminary tests of the assembled probe involved a comparison of the ΔT_{ad} values measured across the T_c of pure gadolinium with the literature data.[26,27] The optimum gadolinium mass deduced from these tests proved to be of the order of 0.2 g. Considering the higher c_p of the alloy,[28–30] with respect to the gadolinium one,[26] a minimum mass of 0.1 g was considered sufficient to perform reliable measurements.

This assumption has been verified while measuring different masses of the same stoichiometry; samples with a mass of 0.15 g were actually used. The error related to the adiabatic temperature change measurement is mainly due to the electric noise of the sensor chip during the experiment.

DSC measurements, carried out on the martensitic phase of the two samples, have been executed with a DSC 821 METTLER TOLEDO driven by STAR^e software. Before performing the experiments, the heat flow, the temperature accuracy, and the tau lag of the instrument were calibrated measuring a reference sample of indium. The heat flow accuracy of the instrument was verified to be ± 1 μW, while the sample signal was about 7 mW.

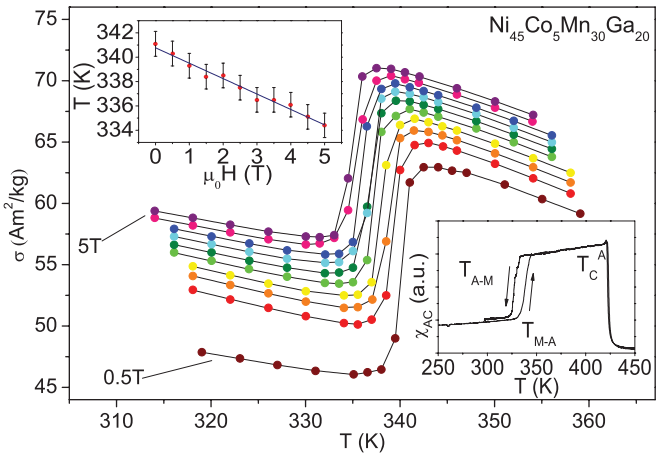

FIG. 2. (Color online) $M(T)$ isofield curves on heating of the martensitic transformation with $0.5 < \mu_0 H < 5$ T on the low ΔM alloy ($Ni_{45}Co_5Mn_{30}Ga_{20}$—*Sample A*) (field step $\mu_0 H = 0.5$ T). Upper inset: T_M vs H phase diagram deduced from isofield curves. Lower inset: ac susceptibility plot showing the martensitic transformation.

III. RESULTS AND DISCUSSION

Sample A, $Ni_{45}Co_5Mn_{30}Ga_{20}$, exhibits a steplike martensitic transformation at 340 K on heating between two ferromagnetic phases (the T_M on cooling being 330 K) (inset of Fig. 2). *Sample B*, $Ni_{41}Co_9Mn_{32}Ga_{16}In_2$, shows, on the other hand, a paramagnetic gap between the Curie transition of martensite ($T_{CM} = 240$ K) and the onset of magnetically ordered austenite (inset of Fig. 3). The latter sample shows large ΔM and $\Delta T_M/\mu_0\Delta H$ values, while the martensitic transformation is temperature-broadened. The partial substitution of 2% Ga with In, while preserving the magnetic critical temperatures,[23] lowers the T_M of the parent quaternary composition $Ni_{41}Co_9Mn_{32}Ga_{18}$ from 436 to 340 K on heating (from 421 to 315 K on cooling). Due to the increased distance between the martensitic transformation and the Curie

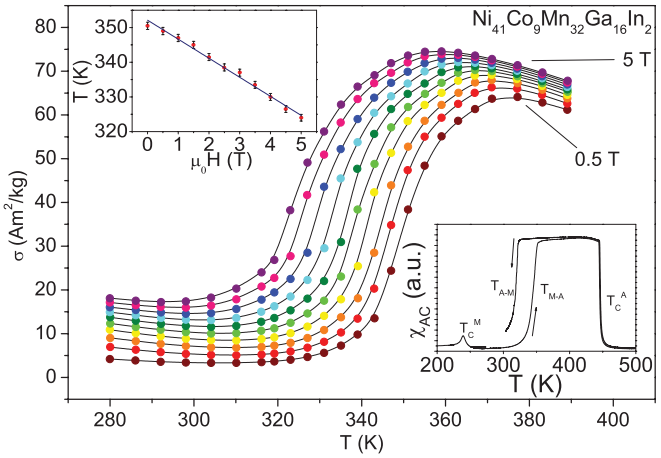

FIG. 3. (Color online) $M(T)$ isofield curves on heating of the martensitic transformation with $0.5 < \mu_0 H < 5$ T on the high ΔM alloy ($Ni_{41}Co_9Mn_{32}Ga_{16}In_2$—*Sample B*) (field step $\mu_0 H = 0.5$ T). Upper inset: T_M vs H phase diagram deduced from isofield curves. Lower inset: ac susceptibility plot showing the onset of the paramagnetic gap.

transition, the ΔM and $\Delta T_M/\mu_0\Delta H$ values (see Table I and Ref. 22) are further improved when compared to the quaternary In-free composition.

It is found that Co substitution of Ni-Mn-Ga alters the relative stability of the martensitic and austenitic structures, hence affecting the transformation temperature. Due to the pronounced dependence of the magnetocaloric properties on temperature, the samples discussed herein are considered representative of the two regimes described above (ferro-ferro and para-ferro martensitic processes) as their transformation temperatures are almost coincident. The lower insets of Figs. 2 and 3 indicate the presence of the thermal hysteresis typical of the first-order martensitic transformation. *Sample A* displays a hysteresis of about 10 K while that of *Sample B* exceeds 25 K. The irreversible nature of the martensitic process manifests itself also as a hysteresis in $M(H)$ curves. The corresponding values have been estimated as about 10 T for *Sample A* and about 5 T in *Sample B*.

A complete isothermal and isofield magnetic characterization has been carried out for the heating martensitic branch of the two samples. The isofield magnetization measurements of *Sample A* at different static magnetic fields up to $\mu_0 H = 5$ T display a first-order transformation around T_M (Fig. 2): the saturation magnetization jump between the two phases reaches $\Delta M = 15 \pm 1$ Am^2/kg, the austenite being the higher moment phase. The same characterization for *Sample B* (Fig. 3) shows a broadened martensitic transformation associated with a remarkable variation of the magnetization ($\Delta M = 60 \pm 2$ Am^2/kg): this is due to the concurrent lowering of magnetic moments in martensite while increasing the austenitic saturation magnetization (M_s). The $\Delta T_M/\mu_0\Delta H$ parameter has been extrapolated by linear fitting the critical temperatures in the (T_M versus H) phase diagram (upper insets of Figs. 2 and 3), built from the isofield magnetization curves. For *Sample B*, a striking value of $\Delta T_M/\mu_0\Delta H = -5.49 \pm 0.18$ K/T is obtained, while for *Sample A*, a value of $\Delta T_M/\mu_0\Delta H = -1.2 \pm 0.07$ K/T is reported (Table I). It is worth noting that the ΔM and $\Delta T_M/\mu_0\Delta H$ measured for *Sample B* turn out to be approximately two and five times the typical values reported for the other Ni-Mn-X compositions, respectively.[6,10,23,31]

$M(H)$ isothermal curves (Figs. 4 and 5) were collected in a field span of $\mu_0 H = 5$ T devoting particular attention to the initial magnetic state before performing each subsequent $M(H)$ measurement. In fact, when dealing with field-induced

TABLE I. Martensitic transformation features and MCE peak values on heating of *Sample A* (without the paramagnetic gap and low ΔM) and *Sample B* (with the paramagnetic gap and high ΔM).

	$\mu_0\Delta H$	*Sample A*	*Sample B*
ΔM (Am^2/kg)		15 ± 1	60 ± 2
$\Delta T_M/\mu_0\Delta H$ (K/T)		-1.2 ± 0.07	-5.49 ± 0.18
$-\Delta s_{isoT}$ (J/Kg K) Cl-Clap		-12.5 ± 1.6	-10.9 ± 0.7
$-\Delta s_{isoT}$ (J/Kg K) Maxwell	2 T	-10.6 ± 1.6	-6 ± 0.8
$-\Delta s_{isoT}$ (J/Kg K) Maxwell	5 T	-13.8 ± 3.3	-9.7 ± 1.9
ΔT_{ad} (K)	1.9 T	-1.05 ± 0.15	-1.6 ± 0.15
RCP (J/kg)	2 T	~30	~100
RCP (J/kg)	5 T	~70	~280

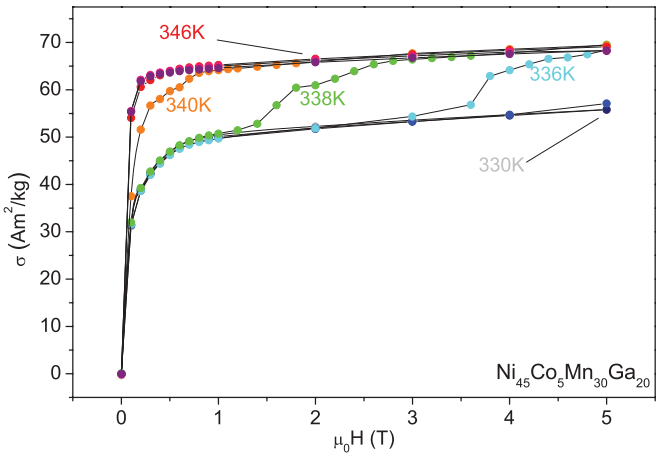

FIG. 4. (Color online) $M(H)$ isothermal curves up to $\mu_0 H = 5$ T performed on the low ΔM alloy ($Ni_{45}Co_5Mn_{30}Ga_{20}$—*Sample A*): $330 < T < 346$ K.

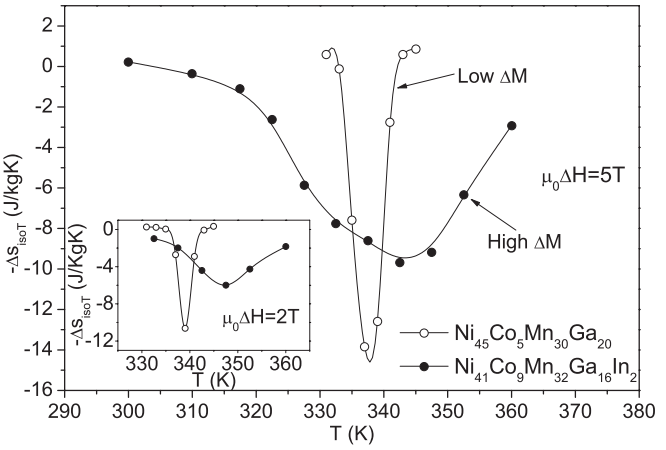

FIG. 6. Comparison between the Δs_{isoT} values of the two different samples, in a $\mu_0 H = 5$ T field span. These values refer to the first-order martensitic transition on heating. Lower inset: Δs_{isoT} curves up to $\mu_0 H = 2$ T. The lines are guides for the eyes.

first-order processes, as in this case, the system could remain partially transformed in the higher magnetization state after removing the saturating field if the cooling martensitic transformation is not crossed.[5,6] In order to avoid this situation, the samples were cooled well below T_M after each isothermal sweep of the magnetic field. In Fig. 6, $\Delta s_{isoT}(T)$ curves are reported for both samples. The data have been calculated by means of the Maxwell relation [Eq. (2)] in field spans of $\mu_0 H = 2$ and 5 T in order to compare, respectively, the first value with the directly measured $\Delta T_{ad}(T)$ data presented in the paper, and the latter with other $\Delta s_{isoT}(T)$ from the literature data. The obtained peak values are compared with the results from the Clausius-Clapeyron equation (1), calculated around both the field- and the temperature-induced transitions. The Clausius-Clapeyron equation is justified in the case of complete magnetic-field-induced transformation. Although for *Sample B* a $\mu_0 H = 5$ T field span is not sufficient to fully induce the martensitic transformation (see Fig. 5), it is still possible to estimate Δs_{isoT} from Eq. (1) if we deduce the ΔM parameter from the $M(T)$ isofield curves. This value, which can also be obtained by extrapolating the $M(H)$ curves of Fig. 5 beyond $\mu_0 H = 5$ T, can be considered a reliable estimation; in fact, the ΔM values calculated both from $M(T)$ and $M(H)$ curves on *Sample A*, where the transformation is fully induced in a 5 T field, are found almost coincident.

In Fig. 7, the ΔT_{ad} as a function of temperature across the first-order martensitic transformation in a field span of $\mu_0 H = 1.9$ T are reported for the two samples. The direct measurements (Fig. 8) were performed taking care of crossing the cooling martensitic transformation after every adiabatic magnetization. Despite the higher Δs_{isoT} peak value of *Sample A*, a remarkable 50% increase of the $|\Delta T_{ad}|$ maximum value is reported for *Sample B*, which shows the paramagnetic gap. *Sample A*, despite its steplike fully induced transformation, shows lower $|\Delta T_{ad}|$ values. Figure 8 shows the two ΔT_{ad} peak values of *Sample A* and *Sample B* as measured by the purpose-built probe: the high signal-to-noise ratio achieved by our setup is clearly visible, the uncertainty of these measurements being of the order of ± 0.1 K. In Table II, the ΔT_{ad} peak values found in the literature around the critical temperatures of several

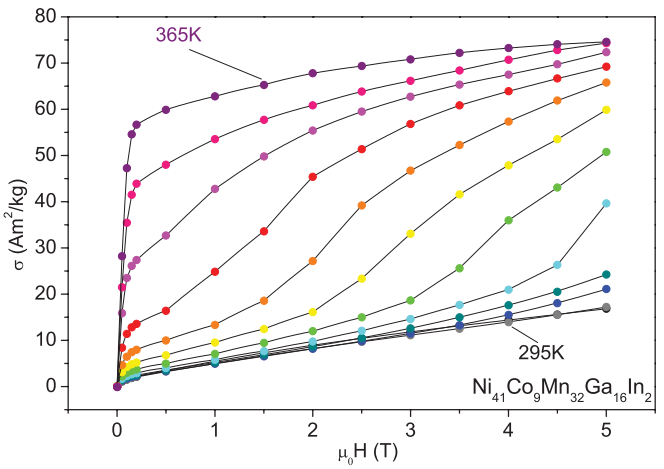

FIG. 5. (Color online) $M(H)$ isothermal curves up to $\mu_0 H = 5$ T performed on the high ΔM alloy ($Ni_{41}Co_9Mn_{32}Ga_{16}In_2$—*Sample B*): $295 < T < 365$ K.

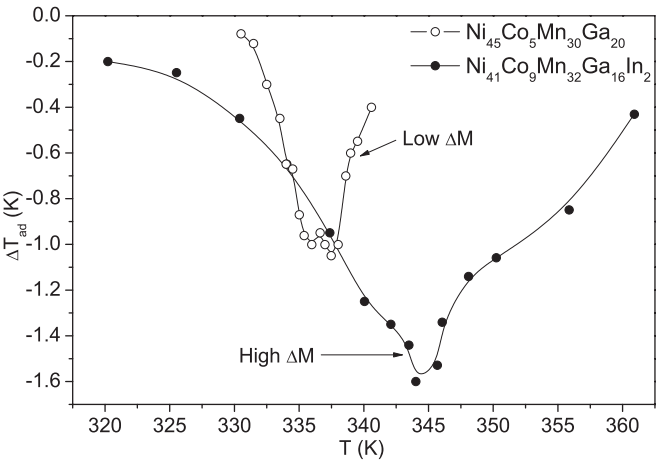

FIG. 7. Comparison between the $\Delta T_{ad}(T)$ of the two different samples in heating, in a $\mu_0 H = 1.9$ T field span. The lines are guides for the eyes.

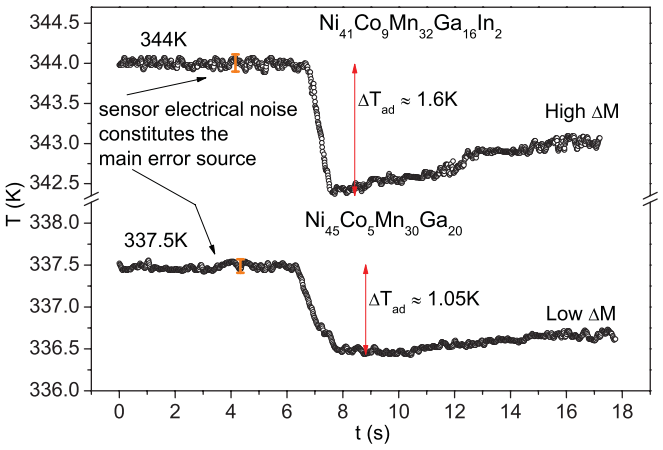

FIG. 8. (Color online) Comparison between the two peak values of $\Delta T_{\rm ad}$ of the two alloys directly measured. It is interesting to compare the field-induced $\Delta T_{\rm ad}$ with the sensor noise, which correspond to the error reported in the paper.

Ni-Mn–based Heusler alloys are compared. Concerning the first-order martensitic transformation on heating reported herein, the value of the quaternary alloy Ni-Co-Mn-Ga (*Sample A*) turns out to be close to most of the literature data, while the In-substituted one (*Sample B*) outreaches it by more than 50%, approaching the best reported values.

As for the temperature domain of the adiabatic temperature jump reported in Fig. 7, *Sample A*, as expected in nearly steplike first-order processes,[3] shows a plateau between 335 and 338 K, which corresponds to the width in temperature of the martensitic transition in $M(T)$ curves, calculated by considering A_s and A_f as the points where the second-order derivative of the $M(T)$ curves shows a maximum and a minimum, respectively. On the other hand, the widening of the martensitic transformation in *Sample B* extends the temperature range ($\sim$10 K) where significant values of $\Delta T_{\rm ad}$ can be exploited.

In the literature, when comparing samples with similar stoichiometries displaying comparable critical temperatures, high $|\Delta T_{\rm ad}|$ are generally expected to correspond with large $\Delta s_{{\rm iso}T}$.[4] However, the difference of the $\Delta T_{\rm ad}$ measured in our two samples does not match with their $\Delta s_{{\rm iso}T}$ calculated by isothermal magnetization measurements (the peak value of $\Delta T_{\rm ad}$ is 50% higher for *Sample B*, while its $\Delta s_{{\rm iso}T}$ peak value is lower both in 2 and 5 T field spans). It appears that the differences between the $\Delta T_{\rm ad}$ peaks are more likely to be connected with different ΔM and $\Delta T_M/\mu_0\Delta H$ values; however, comparing the sensitivities to the applied field of the critical temperatures, while we have the correct indication that *Sample B* is the most promising composition,[3] the difference in the $\Delta T_M/\mu_0\Delta H$ values (-5.48 versus -1.2 K/T) is not reflected in the experimental $\Delta T_{\rm ad}$ values (-1.6 versus -1.05 K).

In order to correlate the main properties of the martensitic transformation, we apply the graphical model reported in Fig. 1 to our measurements. In this qualitative sketch, the slopes of the curves between A_{s-0} and A_{f-0} and A_{s-H} and A_{f-H} provide a mean evaluation (which is only qualitative) of the $c_{p,H}/T$ parameter across the "in-field" martensitic transformation.[4] The "in-field" $s(T)$ curve turns out to be shifted by the applied magnetic field so that

$$(A_{s-0} - A_{s-H}) \approx (A_{f-0} - A_{f-H}) \approx (\Delta T_M/\mu_0\Delta H)\,\Delta H,$$

where $\Delta T_M/\mu_0\Delta H$ is the fitted value up to 5 T reported in Table I.

The samples presented here can be compared by exploiting the relation[1,4,24] $\Delta T_{\rm ad} = -(T/c_{p,H})\Delta s_{{\rm iso}T}$ as the following conditions, in fields up to 2 T, are realized: (i) $A_{s-0} \leqslant A_{f-H}$, so that $c_{p,H}/T = (ds/dT)_H$ is coincident with the hypotenuse DE built on the $\Delta T_{\rm ad}$ and $\Delta s_{{\rm iso}T}$ peak values (see Fig. 1), and corresponds to the slope of the entropy curve directly measurable from calorimetric techniques; (ii) the value of heat capacity far below the transformation is similar between the two samples.[28–30] Considering the diagram of Fig. 1, a proportion between the triangles ABD and the one drawn by the $\Delta T_{\rm ad}$ and $\Delta s_{{\rm iso}T}$ provides

$$AB : \Delta T_{\rm ad} = (\Delta s_{{\rm iso}T} + CB) : \Delta s_{{\rm iso}T}. \qquad (3)$$

Here, $\Delta s_{{\rm iso}T}$ is the peak value calculated from the Maxwell relations in a field span $\mu_0\Delta H = 2$ T, AB is the temperature difference between the two second-order derivative peaks of the $M(T)$ curves corresponding to $\mu_0 H = 0T$ and $2T$ ($A_{s-0} - A_{s-H}$), and $CB' \sim AB\tan\alpha = (A_{s-0} - A_{s-H})\tan\alpha$. The segment BB', which is the contribution of the entropy shift of the martensite under external magnetic field, for $\mu_0\Delta H = 2$ T field span is considered $\sim$0.4 J/Kg K (inset of Fig. 6 and Ref. 6). It has to be emphasized that the above relation for CB' is an approximation. The specific heat before A_s has been measured with a DSC calorimeter and turns out to be about 515 J/kg K for both samples, with an error of 2.5%. This result is in agreement with other literature data.[28–30] From this measurement, $\tan\alpha$ results 1.55 J/Kg K for both *Sample A* and *Sample B*. The values related to a field change of $\mu_0 H = 2$ T are listed in Table III.

The difference between the two $\Delta T_{\rm ad}$ values deduced from this tentative model (in $\mu_0\Delta H = 2$ T) turns out to be $\sim$45%, while the experimentally measured values differ by $\sim$50% in $\mu_0\Delta H = 1.9$ T. The simple construction presented above

TABLE II. $\Delta T_{\rm ad}(T)$ values directly measured across the martensitic first-order transformation (on heating) for different Ni-Mn based Heusler alloys in a $\mu_0 H = 1.9$ T field span. $\Delta T_{\rm ad}(T)$ values related to other transformations (T_M on cooling and T_c) are also listed.

Sample stoichiometry	Ref.	T_M (K)	$\Delta T_{\rm ad}^{\rm heat}$ (K)	$\Delta T_{\rm ad}^{\rm others}$ (K)
$Ni_{47}Mn_{33}Ga_{20}$	32	355	1	
$Ni_{48.3}Mn_{37.5}Sn_{14.2}$	33	314	-0.3[a]	
$Ni_{54.5}Mn_{20.5}Ga_{25}$	34	335	0.8	1.8 ($T_M^{\rm cool}$)
$Ni_{54.75}Mn_{20.25}Ga_{25}$	35	335	0.8	1.2 ($T_M^{\rm cool}$)
$Ni_{50}Mn_{34}In_{16}$	23	225	-1.15	1.6 (T_c)
$Ni_{50}Mn_{34}In_{14}Ga_2$	23	225	-0.75	1.1 (T_c)
$Ni_{50}Co_1Mn_{36}Sn_{13}$	6	295	-1.1	1.15 (T_c)
$Ni_{50}Mn_{35}In_{15}$	36	295	-1.65	1.9 (T_c)
$Ni_{50}Mn_{35}In_{14}Ge$	36	308	-1.54	1.4 (T_c)
$Ni_{50}Mn_{35}In_{14}Al$	36	303	-1.8	1.75 (T_c)
$Ni_{45}Co_5Mn_{30}Ga_{20}$		337	-1.05	
$Ni_{41}Co_9Mn_{32}Ga_{16}In_2$		333	-1.6	

[a]In a $\mu_0 H = 3$ T field span.

TABLE III. Segment values of Fig. 1 for a field change of $\mu_0 H = 2$ T.

Sample	AB (K)	CB (J/Kg K)	$\Delta s_{\mathrm{iso}T}$ (J/Kg K)	$\Delta T_{\mathrm{ad}}^{\mathrm{calc}}$ (K)
$Ni_{45}Co_5Mn_{30}Ga_{20}$	−2.8	4.7	10.6	−1.9
$Ni_{41}Co_9Mn_{32}Ga_{16}In_2$	−10.3	16.3	6	−2.8

gives a more reliable evaluation of the difference between the ΔT_{ad} peak values when compared with the estimation of the same quantity on the basis of the $\Delta T_M/\mu_0\Delta H$ values or the $\Delta s_{\mathrm{iso}T}$ peak values taken alone. An evaluation of the errors linked with the calculated data from Eq. (3) leads to uncertainties of the order of 40%–50%, confirming the qualitative character of this construction. Even if the directly measured ΔT_{ad} peak values are included between the error bars of the calculated ones, they still turn out to be smaller than expected. This gap has already been observed across the first-order process of other magnetocaloric materials.[11,35] Its nature can be partially explained considering several aspects, such as, for instance, the imperfect adiabaticity induced by the finite applying field rate. We have estimated from Fig. 8 that this effect is responsible for a lowering up to 10% of the two directly measured values, allowing for a reduction of the theoretical and experimental spread down under 40%. Therefore, we believe that faster field sweep rates could slightly improve the direct measurement. Another issue involves the reactivity of the magnetostructural transformation to fast field changes. However, it has been shown[35] that the martensitic transformation should be fast enough to respond to the application of the magnetic field even for sweep rates as high as 2 T/s, as in our case. The origin of the reported gap is still an open question. Further studies on the transformation kinetics and on the role of microstructure on the phase boundaries movement should be carried out.

IV. CONCLUSIONS

In conclusion, we report a thorough characterization of the MCE in Ni-Co-Mn-(Ga,In) alloys by exploiting both direct and indirect measurements. The possibility to independently engineer the structural and magnetic critical temperatures of the alloy allows us to achieve remarkably high $|\Delta T_{\mathrm{ad}}|$ values among the Heusler alloys, although significantly lower than those of other reference materials (Gd, Gd-Si-Ge, Mn-As, La-Fe-Si). By inducing the paramagnetic gap, an enhancement of 50% of the adiabatic temperature jump has been realized as compared to the parent composition, which does not display this feature. Therefore, the Ni-Co-Mn-(Ga,In) alloy turns out to be among the most promising Heuslers for magnetocaloric applications.

Future developments in these materials will require, on the one hand, a search for novel compositions characterized by the presence of the paramagnetic gap in order to obtain a further increase of the ΔM and the $\Delta T_M/\mu_0\Delta H$. On the other hand, it will be necessary to understand the role played by the width of the martensitic transformation on the MCE and on the physical parameters affecting it. For instance, a prominent feature affecting the transformation width is the elastic strain set by the structural discontinuity between the two phases.[11] Temperature-dependent structural characterization[37] highlights the fact that the transformation width is linked with the cell volume variation among the martensitic and the austenitic phase (the wider the transition is, the larger is the ΔV). This finding highlights the potential value of studying novel compositions for which such structural discontinuity is enhanced. Concerning the characterization methods commonly employed on the MCE, a seeming discrepancy of the trends connected to the $\Delta s_{\mathrm{iso}T}$ and ΔT_{ad} peak values among different samples has been reported herein. In order to understand this event, a geometrical construction built on the temperature-dependent entropy curves, and accounting for the magnetic features connected to the transformation, is proposed here as a qualitative guide to predict an upper limit of the adiabatic temperature change. The values calculated from this model account for the differences observed among the directly measured peak values. We believe that this model can help to clarify the interplay between the magnetocaloric properties of these systems and the specific-heat behavior. The construction proposed here could also be applied, in principle, to the cooling curves, taking care to coherently change all the parameters. However, additional studies are required in order to understand the origin of the observed discrepancies between the directly measured ΔT_{ad} values and the calculated ones.

ACKNOWLEDGMENTS

The authors thank Dr. M. Mangia and Professor R. Bettini of the "*Group of Pharmaceutical Technology*" of Parma University for the calorimetric DSC measurements.

*giacomo.porcari@nemo.unipr.it

[1] A. M. Tishin and Y. I. Spichkin, *The Magnetocaloric Effect and Its Applications* (Institute of Physics, Bristol, 2003).
[2] K. A. Gschneidner Jr., V. K. Pecharsky, and A. O. Tsokol, Rep. Prog. Phys. **68**, 1479 (2005).
[3] V. K. Pecharsky, K. A. Gschneidner Jr., A. O. Pecharsky, and A. M. Tishin, Phys. Rev. B **64**, 144406 (2001).
[4] V. K. Pecharsky and K. A. Gschneidner Jr., J. Appl. Phys. **90**, 4614 (2001).
[5] L. Caron, Z. Q. Ou, T. T. Nguyen, D. T. Cam Thanh, O. Tegus, and E. Brück, J. Magn. Magn. Mater. **321**, 3559 (2009).
[6] V. V. Khovaylo, K. P. Skokov, O. Gutfleisch, H. Miki, T. Takagi, T. Kanomata, V. V. Koledov, V. G. Shavrov, G. Wang, E. Palacios, J. Bartolom'e, and R. Burriel, Phys. Rev. B **81**, 214406 (2010).
[7] L. Mañosa, A. Planes, and X. Moya, Adv. Mater. **21**, 3725 (2009).
[8] R. Kainuma, Y. Imano, W. Ito, Y. Sutou, H. Morito, S. Okamoto, O. Kitakami, K. Oikawa, A. Fujita, T. Kanomata, and K. Ishida, Nature **439**, 957 (2006).
[9] A. Kitanovski and P. Egolf, Int. J. Refrig. **33**, 449 (2010).
[10] F. Albertini, M. Solzi, A. Paoluzi, and L. Righi, Mater. Sci. Forum **583**, 169 (2008).

[11] A. Planes, L. Mañosa, and M. Acet, J. Phys. Condens. Matter **21**, 233201 (2009).
[12] A. Sozinov, A. A. Likhachev, N. Lanska, and K. Ullakko, Appl. Phys. Lett. **80**, 1746 (2002).
[13] L. Righi, F. Albertini, A. Paoluzi, S. Fabbrici, E. Villa, G. Calestani, and S. Besseghini, Mater. Sci. Forum **635**, 33 (2010).
[14] F. Albertini, L. Pareti, A. Paoluzi, L. Morellon, P. A. Algarabel, M. R. Ibarra, and L. Righi, Appl. Phys. Lett. **81**, 4032 (2002).
[15] K. Ullakko, J. K. Huang, C. Kantner, R. C. O'Handley, and V. V. Kokorin, Appl. Phys. Lett. **69**, 1966 (1996).
[16] M. Kohl, B. Krevet, T. Grund, J. Barth, D. Auernhammer, and F. Khelfaoui, Adv. Sci. Tech. **59**, 119 (2008).
[17] L. Pareti, M. Solzi, F. Albertini, and A. Paoluzi, Eur. Phys. J. B **32**, 303 (2003).
[18] T. Krenke, E. Duman, M. Acet, E. F. Wassermann, X. Moya, L. Mañosa, and A. Planes, Nat. Mater. **4**, 450 (2005).
[19] F. Albertini, A. Paoluzi, L. Pareti, M. Solzi, L. Righi, E. Villa, S. Besseghini, and F. Passaretti, J. Appl. Phys. **100**, 023908 (2006).
[20] S. Y. Yu, Z. X. Cao, L. Ma, G. D. Liu, J. L. Chen, G. H. Wu, B. Zhang, and X. X. Zhang, Appl. Phys. Lett. **91**, 102507 (2007).
[21] S. Fabbrici, F. Albertini, A. Paoluzi, F. Bolzoni, R. Cabassi, M. Solzi, L. Righi, and G. Calestani, Appl. Phys. Lett. **95**, 022508 (2009).
[22] S. Fabbrici, J. Kamarad, Z. Arnold, F. Casoli, A. Paoluzi, F. Bolzoni, R. Cabassi, M. Solzi, G. Porcari, C. Pernechele, and F. Albertini, Acta Mater. **59**, 412 (2011).
[23] S. Aksoy, T. Krenke, M. Acet, E. F. Wassermann, X. Moya, L. Manosa, and A. Planes, Appl. Phys. Lett. **91**, 241916 (2007).
[24] X. Moya, L. Manosa, A. Planes, S. Aksoy, M. Acet, E. F. Wassermann, and T. Krenke, Phys. Rev. B **75**, 184412 (2007).
[25] V. Basso, C. P. Sasso, and M. LoBue, J. Magn. Magn. Mater. **316**, 262 (2007).
[26] S. Yu. Dan'kov, A. M. Tishin, V. K. Pecharsky, and K. A. Gschneidner Jr., Rev. Sci. Instrum. **68**, 2432 (1997).
[27] B. R. Gopal, R. Chahine, and T. K. Bose, Rev. Sci. Instrum. **68**, 1822 (1997).
[28] V. Basso, C. P. Sasso, and M. Kupferling, Rev. Sci. Instrum. **81**, 113904 (2010).
[29] C. P. Sasso, M. Kupferling, L. Giudici, V. Basso, and M. Pasquale, J. Appl. Phys. **103**, 07B306 (2008).
[30] E. Cesari, V. A. Chernenko, J. Font, and J. Muntasell, Thermochim. Acta **433**, 153 (2005).
[31] V. V. Khovailo, V. Novosad, T. Takagi, D. A. Filippov, R. Z. Levitin, and A. N. Vasil'ev, Phys. Rev. B **70**, 174413 (2004).
[32] C. P. Sasso, M. Pasquale, L. Giudici, S. Besseghini, E. Villa, L. H. Lewis, T. A. Lograsso, and D. L. Schlagel, J. Appl Phys. **99**, 08K905 (2006).
[33] M. Pasquale, C. P. Sasso, L. Giudici, T. Lograsso, and D. Schlagel, Appl. Phys. Lett. **91**, 131904 (2007).
[34] V. D. Buchelnikov, V. V. Sokolovskiy, S. V. Taskaev, V. V. Khovaylo, A. A. Aliev, L. N. Khanov, A. B. Batdalov, P. Entel, H. Miki, and T. Takagi, J. Phys. D **44**, 064012 (2011).
[35] V. V. Khovaylo, K. P. Skokov, Y. S. Koshkid'ko, V. V. Koledov, V. G. Shavrov, V. D. Buchelnikov, S. V. Taskaev, H. Miki, T. Takagi, and A. N. Vasiliev, Phys. Rev. B **78**, 060403 (2008).
[36] A. P. Kazakov, V. N. Prudnikov, A. B. Granovsky, A. P. Zhukov, J. Gonzalez, I. Dubenko, A. K. Pathak, S. Stadler, and N. Ali, Appl. Phys. Lett. **98**, 131911 (2011).
[37] F. Albertini, S. Fabbrici, A. Paoluzi, J. Kamarad, Z. Arnold, L. Righi, M. Solzi, G. Porcari, C. Pernechele, D. Serrate, and P. Algarabel, Mater. Sci. Forum **684**, 151 (2011).